

# Image-based classification of skin cancer using convolution neural network

Priotosh Mondal  
Department of Computer Engineering  
VES Institute of Technology  
Mumbai, India  
2020.priotosh.mondal@ves.ac.in

Aditi Bhatia  
Department of Computer Engineering  
VES Institute of Technology  
Mumbai, India  
2020.aditi.bhatia@ves.ac.in

Roshini Panjwani  
Department of Computer Engineering  
VES Institute of Technology  
Mumbai, India  
2020.roshini.panjwani@ves.ac.in

Shrey Panchamia  
Department of Computer Engineering  
VES Institute of Technology  
Mumbai, India  
2020.shrey.panchamia@ves.ac.in

Indu Dokare  
Department of Computer Engineering  
VES Institute of Technology  
Mumbai, India  
indu.dokare@ves.ac.in

**Abstract**—Skin cancer is a category or collection of cancer affecting the tissues and layers of skin. Skin cancer is classified into several types depending on the type of cell it affects. These types include melanoma, melanocytic nevus, basal cell carcinoma, benign keratosis, actinic keratosis, dermatofibroma, vascular lesion, and squamous cell carcinoma. Melanoma which affects the melanocytes and is considered to be the most fatal and deadly cancer, is growing at an alarming rate, especially in the western hemisphere and the Pacific region. The proposed system contained a web-based application where the image of an affected skin area can be uploaded and the likelihood of skin cancer is displayed. This system has used a convoluted neural network (CNN) based binary and multi-classification model making efficient use of image processing, computer vision, OpenCV, and Python to classify dermatoscopic lesion images into cancerous and non-cancerous along with their types. The implemented binary classifier achieves an accuracy of 92%. Further, the multi-class classification model is implemented based on CNN to classify dermatoscopic cancerous lesion images into nine types which achieved an accuracy of 97%. Among nine classes one of the classes is non-cancerous. The models aim to provide a means of diagnostic tool that will help in the preliminary diagnosis of skin lesions. Early detection and diagnosis are appropriate measures to combat the spread and lethality of skin cancer.

**Keywords**—Skin cancer, Image classification, CNN, OpenCV

## I. INTRODUCTION

Skin cancer is a highly prevalent and often fatal form of cancer. While melanoma is less common than other skin cancers, it has a higher propensity to spread to surrounding tissue and other parts of the body. Melanoma originates in melanocytes, which are located in the basal layer of the epidermis and produce melanin, a pigment that absorbs UV radiation [15], [16]. When keratinocytes in the epidermis are exposed to UV radiation, they produce a hormone that stimulates melanin production in melanocytes. The melanin is then transferred to surrounding keratinocytes, which accumulate and forms a protective barrier against the harmful effects of UV radiation.

Overexposure to UV radiation is a significant risk factor for skin cancer, as it can damage the DNA in skin cells and trigger melanin production. The World Health Organization has identified long-term and repeated exposure to UV radiation as the main cause of benign melanoma, and

decreasing latitude is also associated with a higher risk of skin cancer due to increased UV radiation levels. To prevent skin cancer, it is important to limit exposure to UV radiation by using protective clothing, and sunscreen and avoiding indoor tanning. Regular skin examinations can also help detect skin cancer early for prompt treatment [17].

Malignant melanoma is more prevalent in individuals with fair skin, blue eyes, and blond or red hair. The primary risk factors for melanoma are excessive and sporadic exposure to UV radiation from the sun, a personal or family history of melanoma, extended use of tanning beds, a significant number of abnormal moles, and a weakened immune system. Melanocytes produce two types of melanin: eumelanin, which is a blackish-brown pigment, and pheomelanin, which is a reddish-yellow pigment. The ratio of these two pigments influences skin colour, with those having darker skin having a higher UV protection barrier because of eumelanin. Conversely, individuals with more pheomelanin are at a higher risk of skin cancer because it creates carcinogens and damages DNA more severely in response to UV radiation. The risk of melanoma is directly linked to skin, hair, and eye colour, with individuals who have lighter skin that does not tan, blond or red hair, and light eyes being more susceptible to developing melanoma than the general population [15].

The MC1R gene regulates skin, hair, and eye colour. Eumelanin production is stimulated by a fully functional MC1R. Due to greater exposure of nuclei to UV radiation, individuals with less functioning versions of MC1R accumulate more mutations. Skin malignancies develop when mutations build up in vulnerable areas of the genome [18].

They mostly develop in areas which are exposed to the sun such as the legs, hands, and face. Melanomas can also occur in areas that don't receive much sun exposure, such as the soles of your feet, palms of your hands and fingernail beds. These hidden melanomas are more common in people with darker skin. A change in the existing mole or the development of new pigmented or unusual-looking growth on the skin can be a major symptom of melanoma [18].

Several characteristics of melanoma include a big brown patch with darker speckles and a mole that bleeds. This patch can vary in size, colour and texture. The ABCDE examination method is widely used for visual inspection of whether a mole could be cancerous or not.

Melanomas are usually asymmetric, the edges are ragged. They are of uneven shades of various colours like brown, red, tan, white and even blue. The diameter of melanomas is greater than 6 millimetres and the mole feels itchy and bleeds occasionally [15]. Another method that can be used is Biopsy or Ugly-duckling in which a correlation of common lesion characteristics is made and the lesions that deviate from the common characteristics are labelled "Ugly Duckling" [19].

Skin cancer is majorly divided into eight classes: Melanoma, Actinic Keratosis, Vascular Lesion, Basal Cell Carcinoma, Benign Keratosis, Squamous Cell Carcinoma, Melanocytic Nevus and Dermatofibroma.

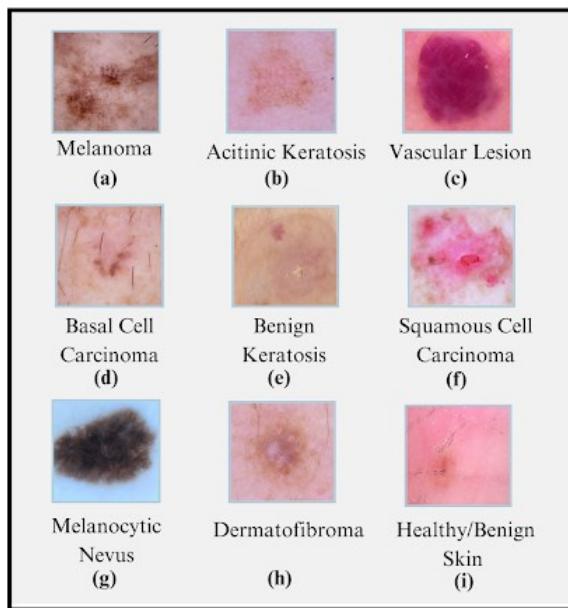


Fig. 1. Skin cancer types from ISIC 2019 dataset

**Melanoma:** Melanoma as shown in Fig. 1(a) is the most serious type of skin cancer and is most often developed in areas which are more exposed to the sun like the face, arms, back and legs. Melanoma is an unusual growth in the skin with irregular symmetry, boundaries and colouration [15].

**Actinic keratosis:** Fig.1(b) presents Actinic keratosis which is also known as solar keratosis as it is developed over the years due to sun exposure. It is often developed around the face, lips, ears, forearms, scalp and neck and looks like a rough scaly patch which is itching, burning or bleeding [20].

**Vascular lesion:** Vascular lesions are common abnormalities of the skin and underlying tissues as seen in Fig. 1(c). They are commonly found on the head and neck. Most of these lesions are congenital but some may be cancerous. The most common type of vascular lesions are bright red in colour; it fades and shrinks over time but can also cause a permanent mark [21].

**Basal cell carcinoma:** Basal cell carcinoma usually looks like a transparent bump on the skin as seen in Fig. 1(d) which is most exposed to sunlight like the face and arms as it is caused due to harmful long-term exposure to ultraviolet radiation. It can also look like a dark-coloured lesion with a translucent border, a scaly patch on the skin or a white scar-like lesion [22].

**Benign keratosis:** Benign keratosis is also known as seborrheic keratosis and is a common non-cancerous skin growth shown in Fig. 1(e). People tend to get more of them as they get older. They are brown, tan or light tan in colour and have a waxy or scaly patch [23].

**Squamous cell carcinoma:** Squamous cell carcinoma depicted in Fig. 1(f) is a common type of skin cancer that develops in squamous cells. It can be aggressive, grow in size, and spread to other parts of the body, leading to severe complications. The main cause of such a cancer is prolonged exposure to ultraviolet radiation. The lesions are often red in colour and may be scaly and crusty [15].

**Melanocytic Nevus:** Melanocytic nevus shown in Fig. 1(g) develops in the nevus cells. They are usually skin tags, raised moles or flat moles. Benign moles are usually tan, brown, pink or black in colour, circular in shape and smaller in size, unlike melanoma [24].

**Dermatofibroma:** Dermatofibroma as shown in Fig. 1(h) is seen in adults and is more common in women than in men. They can sometimes be caused due to minor injuries like insect bites, injections, and rose thorn injuries and can also be caused in patients suffering from HIV and autoimmune diseases. It can occur anywhere on the skin and its colour varies from pink to light brown in white skin and dark brown to black in dark skin. They can be painful, itchy or tender [25].

Effective treatment and better outcomes for skin malignancies depend on early identification. Specialists are capable of precisely diagnosing cancer, but due to their scarcity, it is necessary to create automated systems that can do it quickly and effectively. This will help save lives and lessen the financial and medical burdens placed on patients. It can be challenging to distinguish between benign skin lesions and skin malignancies because melanoma has a wide range of appearances. Artificial Intelligence and Machine learning can help with early skin cancer identification, reducing the morbidity and mortality burden of the condition [28]. AI and ML-based technologies can aid by lowering workload and enhancing skin lesion diagnosis

A lot of efforts have been taken to develop machine learning algorithms to accurately detect skin cancer but a lot of these fail because of the scarce dataset and a smaller number of classes taken into account by them and they couldn't classify the lesions into the type of skin cancer, they could only predict whether the lesion could be cancerous or not.

There are various non-invasive imaging methods and tools available to detect skin cancer or abnormalities in the skin. Several smartphone applications, including SkinVision [13], UMSkinCheck [13], and MoleScope [13], have been created with the stated intentions of enabling widespread accessibility, lowering the cost of screening, and eventually improving patient early detection. Two devices, MelaFind [14] and SIAScope [14] use visible and near-infrared light to visualise lesions and give information to help clinicians decide whether a biopsy is necessary, these tools help the patient for early detection but aren't that accurate and often give false predictions.

This proposed system aims to create an application that uses advanced image processing techniques powered by AI and machine learning to help people detect skin cancer and its variants. The model will allow users to analyse real-time

images of abnormal skin spots to determine the likelihood of skin disorders being cancerous or non-cancerous, which can then be discussed with medical professionals to receive appropriate treatment, the web-based application also provides information regarding the different types of skin cancer, their diagnosis, treatment and symptoms.

Hence, this proposed system can be a useful tool for medical practitioners, researchers, and experts in the field of oncology and dermatology to detect and prevent skin cancer in its early stages.

The next part of the paper goes as follows: Section II explains the related work used in this study, and Materials and methods are demonstrated in section III. Section IV reports the results and discussion whereas section V covers the conclusion.

## II. RELATED WORK

The research of skin cancer detection based on the analysis of dermoscopic images has advanced significantly over the years. Melanoma is classified as either benign or malignant in a majority of research work done for the identification of melanoma using various machine learning algorithms. The ISIC 2019 dataset and ABCD and GLCM method for feature extraction is used in [1]. Colour-based k-means clustering is performed in the segmentation phase and Multiclass SVM was used for the classification of skin cancer as benign and malignant. The work proposed by [2] used the ISIC 2020 dataset containing about 5341 images. It used the ABCD method for feature extraction and SVM for classification purposes. The model developed was then evaluated using specificity, accuracy and sensitivity. An accuracy of 95% was obtained using deep CNN classification methods and the ISBN dataset in [3]. SNN methods for classification used in [4] achieved an overall accuracy of 87.7% with a better runtime accuracy than CNNs. SNNs are more stable, easy to use and reliable as compared to pre-trained CNNs. The research study outlined in [5] employed a lightweight skin cancer recognition model with feature discrimination based on fine-grained classification principles. The suggested model contained two similar lesion categorization networks and feature discrimination network feature extraction modules and achieved an accuracy of 96.2%. A simple approach implemented by [6] has taken a coloured image as an input, resize the image to extract features using pre-trained CNN models and then classified the features using multiclass SVM that could detect 3 types of skin diseases with 100% accuracy. A new intelligent system based on several neural networks connected on two levels of classification proposed in [8] showed that the use of the objective classifier brings an accuracy of 97.5% and F1 score of 97.47%. A deep learning studio to develop intelligent data discovery models was used in [9]. Using standard datasets, the developed deep-learning models were tested, and a performance metric area under the curve of 99.77% was obtained. The classification was performed using a combination of coloured and grey scaled images in [12] and the k-means algorithm was used for segmentation and ABCD method. it produced findings that were better and more precise. They achieved an average accuracy of 70%.

The next section describes the materials and methods used for the implementation of the system.

## III. MATERIALS AND METHODS

### A. Dataset Description and Preparation

The proposed system has used ISIC 2019 dataset obtained from the official ISIC challenge website [26] for skin cancer images and the healthy skin images are obtained from the SIIM-ISIC melanoma classification dataset available on the official ISIC challenge website [27]. The ISIC 2019 dataset contains skin lesion images for eight types of skin cancers such as melanoma, melanocytic nevus, basal cell carcinoma, actinic keratosis, benign keratosis, dermatofibroma, vascular lesion, and squamous cell carcinoma.

This dataset contains a total of 25,331 images of skin cancers. Whereas 1000 images of healthy/benign skin obtained from SIIM-ISIC are used in this implementation.

For dataset preparation as shown in fig. 2, we have divided the entire ISIC 2019 dataset into different folders according to the type of skin lesion using the labels provided in the dataset. The ninth folder contains 1000 healthy/benign skin images obtained from the SIIM-ISIC dataset.

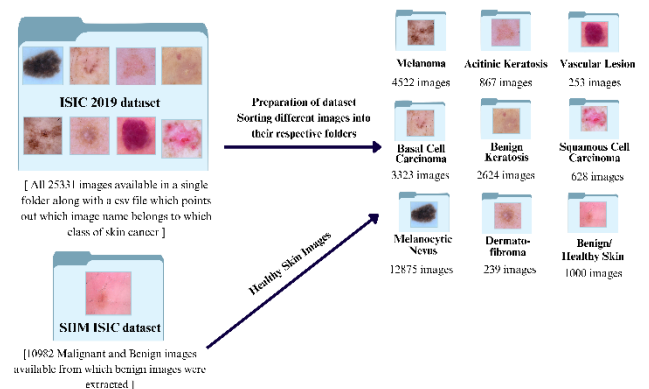


Fig. 2. Dataset preparation

### B. Proposed System

The proposed system as shown in Fig. 3 is a web-based application that helps in the early diagnosis of skin cancer. Any user who wants to check any skin anomaly present can upload an image on the website for cancer detection purposes. The user can select if they want to use the binary classification or multi-classification model which is deployed. They will upload an image following the guidelines specified on the web page and then click on upload. The image uploaded will then be pre-processed to remove any disturbances like noise and hair using Morphological black hat transformation and the inpainting algorithm this is done because skin cancer images can contain various disturbances, such as hair, dust, or shadows, which can interfere with the accuracy of the diagnosis. Now if the user had selected binary classification the image will be classified as Melanoma or non-Melanoma/Normal, and for multi-classification, the image will be categorised as one of the nine classes and the likelihood of each class will be displayed in the form of a percentage of chance of occurrence. The user can also learn more about the different categories of skin cancer their symptoms, diagnosis, causes risk factors and the treatment available.

This proposed system contributes as follows:

- The proposed system accepts an image for cancer detection purposes.
- The image noise removal and hair image removal are implemented using Morphological black hat transformation and the Inpainting algorithm.
- The binary image classification and multi-class classification are employed using convolution neural networks.
- It can be used for binary image classification by selecting a respective option where the uploaded image can be categorised as cancerous or non-cancerous.
- If the multiclass classification option is selected, then the system classifies an image into one of the categories with its likelihood of occurrence among others

Fig. 4. describes the CNN model in the proposed system. The dataset along with its labels was given as input to the model. Data Augmentation techniques like rotation and flipping of images were applied to increase the size and balance the training dataset by creating new variations of existing data. This helps to reduce overfitting and improve the generalization ability of the model. The data was pre-processed by removing noise and hair from the dataset and then fed to the CNN Classifier. The CNN classifier consisted of 6 pairs of convolutional and pooling layers followed by a flattening and two dense layers. Both binary and multi-class classification is done, Binary classification classifies the image as Melanoma or Non-Melanoma/Normal, and Multiclass classification classifies the image into nine categories. The labels were extracted using the Pandas Python library and accordingly, the dataset was segregated into eight categories.

#### 1) Data Preprocessing

It is necessary to deal with noise in the image and enhance the quality of the image before classification to improve the accuracy of the model. It is essential to use it to restrict the search for anomalies in the background factors influencing the outcome. The following methods are used for noise and hair removal.

##### a) Morphological Black Hat Transformation:

This technique is used to enhance certain features of an image and can be useful in applications such as image segmentation, edge detection, and feature extraction. Skin cancer images often contain various types of features, such as irregular shapes, colours, and texture patterns, that are not always easy to detect. By applying a morphological black-hat transformation, the smaller and more subtle features of the skin cancer images can be enhanced, making it easier for identification.

$$B(x, y) = C(x, y) - I(x, y) \quad (1)$$

$B(x, y)$  is the output image,  $C(x, y)$  is the closing of the input image  $I(x, y)$ , and  $(x, y)$  are the pixel coordinates. The closing of an image  $I(x, y)$  is defined as the dilation of the erosion of the image by a structuring element SE.

##### b) Inpainting Algorithm:

The Inpainting algorithm is an image restoration technique used to fill in missing or damaged parts of an image. It involves using information from the surrounding pixels to estimate the missing pixels and fill them in. Skin cancer images can also contain various disturbances, such as hair, dust, or shadows, which can interfere with the accuracy of the diagnosis. By applying an Inpainting algorithm, they can be removed or restored, reducing their impact on the analysis and increasing the accuracy of the diagnosis.

#### 2) Feature Extraction Methods

Feature extraction is the technique employed to extract important characteristics from dermoscopy images. The ABCD rule of dermoscopy pictures is used because of its efficacy, efficiency, and ease of implementation and execution. The ABCD rules are defined as follows:

##### a) Asymmetry:

The lesion area is divided into two subregions based on the longest diagonal  $d$  calculated using the Euclidean distance formula.

$$d = (x_2 - x_1)^2 + (y_2 - y_1)^2 \quad (2)$$

$(x_1, y_1)$  and  $(x_2, y_2)$  are pixels present on the border of the lesion. All pixels on the border are analysed to find the pair having the largest distance between them. Similarities between the two sub-regions are analysed by calculating perpendicular distances between the boundary pixels having a distance greater than  $d$ .

##### b) Border:

Pixels present at the boundary obtained due to segmentation of the lesion are border pixels. The lesion is divided into eight parts equally and portions with a discontinuous or uneven cut are calculated. A regular part of the skin gives a value of 0, an irregular part gives a value of 1 and the degree of melanoma varies from 3 to 8. Vector product descriptors and inflexion point descriptors are used to extract irregular boundaries, lines exhibiting a change in direction, and irregular peaks and valleys.

##### c) Colour:

Colour is one of the most important features, the six colours: white, red, light brown, dark brown, blue-grey and black are to be considered. The browns represent the melanin located in the epidermis, black is for the melanin in the upper granular layer of the epidermis. The blue-grey is for the melanin in the papillary dermis, the white is for areas of regression and the red represents the degree of inflammation. The presence of any one of the above colours increases the colour score by 1.

##### d) Diameter:

If a skin lesion has a diameter greater than 6mm, it indicates that the lesion is most likely malignant. The diameter is the maximum distance between two boundary pixels of the lesion, the diameter score is added by one for every 1mm.

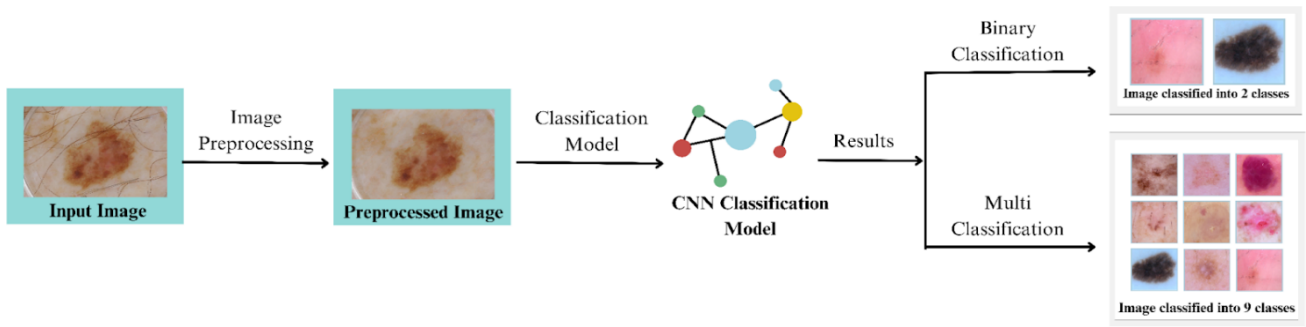


Fig. 3. Proposed system for skin cancer classification

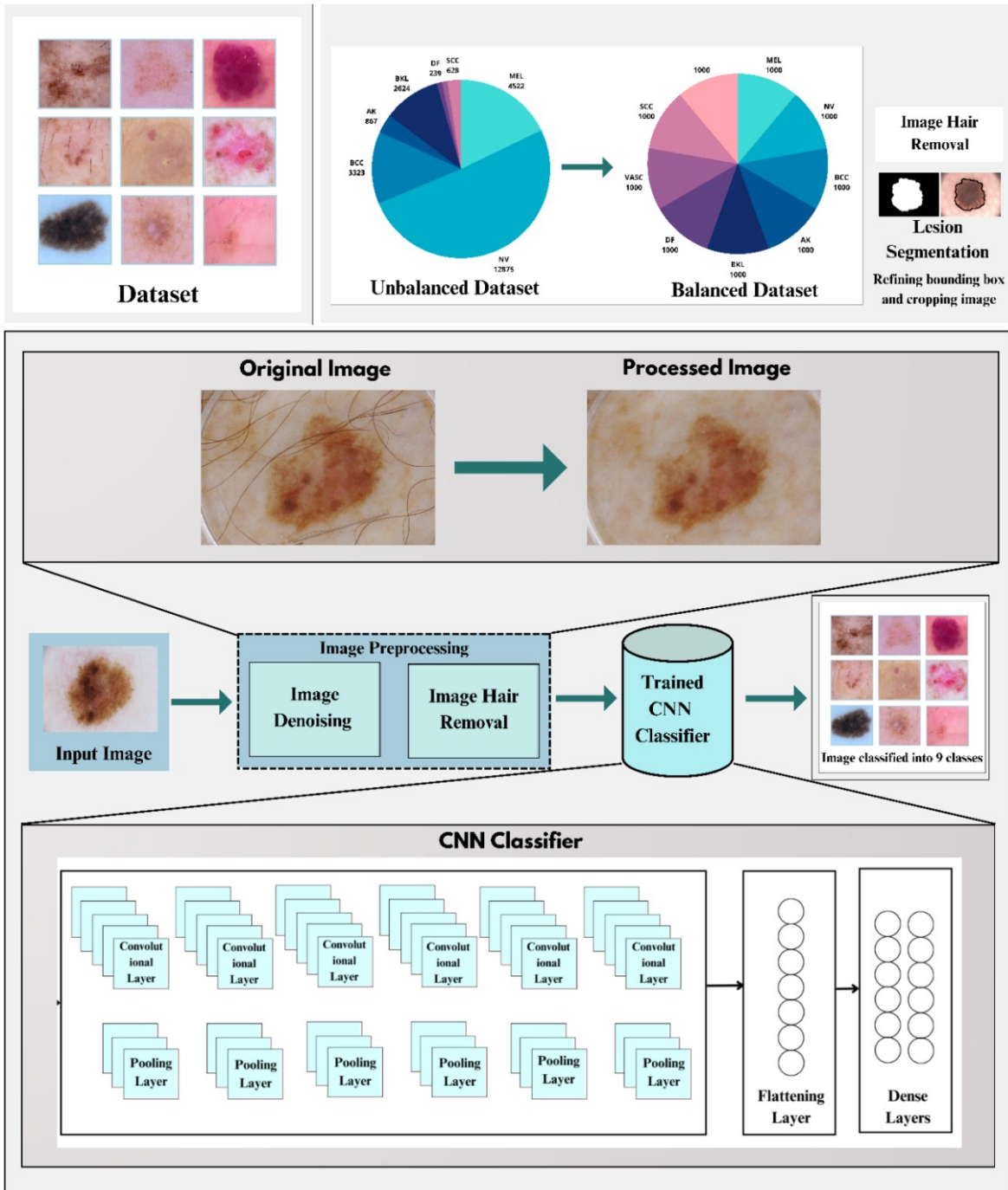


Fig. 4. Proposed CNN-based classification model



### 3) CNN Model

A subset of deep learning neural networks is the convolutional neural network. They are typically employed in the background of picture categorization and are most usually utilised to analyse visual imagery. The structure of CNN is the same as that of neural networks in general, and its neurons have the functions of weight, bias, and activation. The feature extraction layer of CNN's architecture is made up of a pooling layer, a convolution layer with ReLu activation, and a fully connected layer with softmax activation as the classification layer

Convolutional layers make up CNN's first layer, and they include the following parameters: (filters=32, padding="same", kernel size=3, activation="ReLU", "strides=2, and input shape = [100,100, 3]). A CNN may contain several convolutional layers. The input for the first convolutional layer is the images, which it then starts to process. This layer aims to retain associations between nearby pixels while extracting a set of features from the image. A pooling layer makes up the second layer. In a CNN, there may be several pooling layers. A pooling layer is followed after each convolutional layer. As a result, convolution and pooling layers are applied in tandem. The pooling layer serves a variety of functions, such as extracting the most significant (relevant) features by obtaining the greatest number or averaging the numbers, decreasing the dimensionality (number of pixels) of the output returned by earlier convolutional layers, and minimising the number of parameters in the network.

Features are extracted from the image using a combination of convolutional and pooling layers. The multi-class classifier uses 6 pairs and the binary classifier only uses 4 pairs of convolutional and pooling layers. The next layer is known as the flattening layer. The final pooled feature map output from the last pooling layer is sent to a Multilayer Perceptron (MLP) in a CNN, which can categorise the output into a class label. Data can only be one dimension for an MLP. Hence, images from the final pooled feature map are flattened into a single column that contains the input information for the MLP. Important pixel dependencies are kept when pooled maps are flattened, unlike when the original image is flattened. The dense layers are the last two layers. These layers receive the output from the flattening layer and classify it. For binary classification, a linear activation function is employed. This parameter's linear setting produces outcomes resembling those of an SVM classifier. The last layer has also been given an l2 regularizer. During optimization, regularizers let you impose penalties on layer parameters or layer activity. The loss function that the network optimises includes the total of these penalties. For multi-class classification, the softmax activation function is used

### 4) Website Flow

According to Fig. 5, the user will be able to select the binary or multi-classifier according to their need from the home page. They will also be able to view information about the type of skin cancers, their diagnosis, symptoms, treatment and risk factors. After selecting the type of classifier, the user will then upload an image. The image will get denoised and the hair will be removed then the image will be classified as cancerous or non-cancerous if the user selects a binary classifier, and the likelihood of nine types of cancer if the user selects a multi-class classifier.

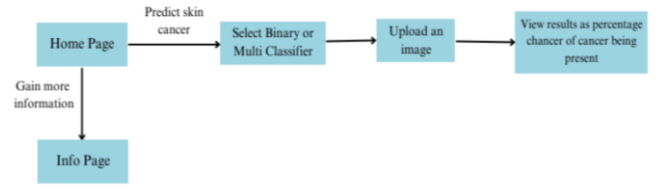


Fig. 5. Website flow of the proposed skin cancer classification system

### 5) Performance Measures

A confusion matrix is a performance measurement tool used in the process of evaluation of Machine learning models where the output can be of 2 or more classes. It is extremely useful for measuring Recall, Precision, Specificity, Accuracy, and most importantly AUC-ROC curves.

**True Positive (TP):** The sample is correctly predicted as positive.

**True Negative (TN):** The sample is correctly predicted as a negative.

**False Positive (FP):** The sample is incorrectly predicted as positive.

**False Negative (FN):** The sample is incorrectly predicted as negative

TABLE I. PERFORMANCE MEASURES

Accuracy	$(TP+TN)/(P+N)$ (3)
Precision	$(TP)/(TP+FP)$ (4)
Sensitivity	$(TP)/(TP+FN)$ (5)
Specificity	$(TN)/(TN+FP)$ (6)
Recall	$(TP)/(TP+FN)$ (7)

## IV. RESULTS AND DISCUSSION

The implementation of two classifiers includes the binary classifier, which determines if the input image is cancerous or benign, and the multiclass classifier, which classifies the image into nine classes.

A seven layers CNN model as shown in Fig.6. works as an automatic feature extractor and a binary classifier. The seven layers are formed through a combination of convolutional layers, pooling layers, flattening, and dense layers, each of which is assigned and performs a different function in the pipeline. The activation of the last dense layer is set to linear which makes the model behave in a fashion similar to SVM classifiers. The model extracts features from the training dataset using CNN and passes these learned features to the CNN classifier to classify the images into melanoma and non-melanoma. When we use a Linear activation in the final dense layer for binary classification. It yields results similar to implementing a Linear SVM model.

The 16-layered CNN multi-classifier classifies lesion images into 9 classes: Actinic Keratosis, Benign Keratosis, Melanoma, Basal Cell Carcinoma, Squamous Cell Carcinoma, Dermatofibroma, Melanocytic Nevus, Vascular Lesion, and Healthy Skin.

The multiclass classifier as shown in Fig. 8. helps to detect the type of skin cancer and the accuracy of the prediction for all the classes. The dataset which consisted of 25,000 images was imbalanced, thus data augmentation was performed by flipping and rotating the images and it was converted into a dataset of 1000 images to make it balanced and to avoid overfitting of the data. For multiclass classification, we use softmax as an activation function for the final dense layer of the CNN model. Compared to other models, CNN models are proven to show a significant improvement in terms of accuracy, precision, and recall. The results obtained by the proposed system are discussed ahead.

#### A. CNN Binary Classification Results

Model: "sequential_1"		
Layer (type)	Output Shape	Param #
conv2d_4 (Conv2D)	(None, 100, 100, 32)	896
max_pooling2d_4 (MaxPooling 2D)	(None, 50, 50, 32)	0
conv2d_5 (Conv2D)	(None, 50, 50, 32)	9248
max_pooling2d_5 (MaxPooling 2D)	(None, 25, 25, 32)	0
conv2d_6 (Conv2D)	(None, 25, 25, 32)	9248
max_pooling2d_6 (MaxPooling 2D)	(None, 12, 12, 32)	0
conv2d_7 (Conv2D)	(None, 12, 12, 32)	9248
max_pooling2d_7 (MaxPooling 2D)	(None, 6, 6, 32)	0
flatten_1 (Flatten)	(None, 1152)	0
dense_2 (Dense)	(None, 128)	147584
dense_3 (Dense)	(None, 1)	129
Total params: 176,353		
Trainable params: 176,353		
Non-trainable params: 0		

Fig. 6 Binary classifier CNN model layer description

The model requires input images to have a size of 200x200 with RGB channels. The first 8 layers consist of Conv2D and MaxPooling2D layers, which extract features from the input image. These Conv2D layers use 3x3 filters with 32 filters to extract different levels of features. The MaxPooling2D layers reduce the output spatial dimensions of the Conv2D layers by taking the maximum value in each 2x2 pool. Next, a Flatten layer transforms the output of the previous layer into a 1D vector. Two Dense layers follow, with 128 and 8 units, respectively. The last layer has 1 unit, which is one less than the total number of classes that the model is trained to classify.

		Confusion Matrix	
		0	1
Actuals	0	1643	138
	1	215	1566
		Predictions	

Fig. 7. Confusion Matrix for binary classification

0: Non Melanoma 1: Melanoma

The results calculated from the confusion matrix Fig. 7 obtained from the binary classification model are summarized in Table II. The 11-layered CNN binary classifier Fig. 6 which classifies lesion images into Melanoma/Non-Melanoma produced the following results when evaluated with a testing dataset of 3562 unlabeled images.

TABLE II. RESULTS FOR BINARY CLASSIFICATION MODEL

Parameter	Value (%)
Accuracy	92.08
Precision	88.42
Sensitivity	92.25
Specificity	87.92
Recall	92.20

As shown in table II, an accuracy is the percentage of correct predictions for the test data. The accuracy obtained is 92.08% which is similar to existing works. Precision of the proposed model recorded is 88.42%. The sensitivity of the model is 92.25% which is better than the existing work reported in this study. The proposed model achieved the specificity and recall of 87.92% & 92.2% respectively. The training data of 10982 images & testing data of 3562 images used in this work is relatively larger than dataset used in existing works, hence the results obtained by the proposed work are highly satisfactory.

## B. CNN Nine-Class Classification Results

Model: "sequential"		
Layer (type)	Output Shape	Param #
rescaling (Rescaling)	(None, 200, 200, 3)	0
conv2d (Conv2D)	(None, 200, 200, 16)	448
max_pooling2d (MaxPooling2D)	(None, 100, 100, 16)	0
conv2d_1 (Conv2D)	(None, 100, 100, 16)	2320
max_pooling2d_1 (MaxPooling2D)	(None, 50, 50, 16)	0
conv2d_2 (Conv2D)	(None, 50, 50, 32)	4640
max_pooling2d_2 (MaxPooling2D)	(None, 25, 25, 32)	0
conv2d_3 (Conv2D)	(None, 25, 25, 32)	9248
max_pooling2d_3 (MaxPooling2D)	(None, 12, 12, 32)	0
conv2d_4 (Conv2D)	(None, 12, 12, 64)	18496
max_pooling2d_4 (MaxPooling2D)	(None, 6, 6, 64)	0
conv2d_5 (Conv2D)	(None, 6, 6, 64)	36928
max_pooling2d_5 (MaxPooling2D)	(None, 3, 3, 64)	0
flatten (Flatten)	(None, 576)	0
dense (Dense)	(None, 128)	73856
dense_1 (Dense)	(None, 8)	1032
Total params: 146,968		
Trainable params: 146,968		
Non-trainable params: 0		

Fig. 8 Nine-class classifier CNN model layer description

The input images are expected to be 200x200 RGB images. The first layer is a Rescaling layer that scales the pixel values of the image between 0 and 1.

The next 12 layers are Conv2D and MaxPooling2D layers that extract features from the input image. The Conv2D layers use 3x3 filters with different numbers of filters (16, 32, and 64) to extract different levels of features. The MaxPooling2D layers reduce the spatial dimensions of the output of the Conv2D layers by taking the maximum value in each 2x2 pool. Then a Flatten layer flattens the output of the previous layer to a 1D vector. Two Dense layers follow, with 128 and 8 units respectively. The last layer has 8 units, which is one less than the number of classes that the model is trained to classify.

		Confusion Matrix								
		0	1	2	3	4	5	6	7	8
Actuals	0	86	4	3	2	1	0	1	4	0
	1	3	92	2	2	0	0	0	2	0
	2	1	1	80	1	0	2	15	1	0
	3	0	6	1	89	1	0	1	3	0
	4	1	0	2	1	92	1	3	1	0
	5	0	1	0	0	0	95	3	2	0
	6	0	1	2	0	1	13	83	1	0
	7	3	2	0	1	1	0	2	92	0
	8	0	0	0	1	1	0	0	0	99
		Predictions								

Fig. 9. Confusion Matrix for multi-class classification

0: Actinic Keratosis, 1: Basal Cell Carcinoma, 2: Benign Keratosis, 3: Dermatofibroma, 4: Healthy Skin, 5: Melanocytic Nevus, 6: Melanoma, 7: Squamous Cell Carcinoma, 8: Vascular Lesion

The 16-layered CNN binary classifier classifies lesion images into 9 classes: Actinic Keratosis, Benign Keratosis, Melanoma, Basal Cell Carcinoma, Squamous Cell Carcinoma, Dermatofibroma, Melanocytic Nevus, Vascular Lesion, and Healthy Skin as shown in Fig. 8. The results calculated from the confusion matrix Fig. 9 obtained from the model are summarised in Table III.

TABLE III. RESULTS FOR MULTI-CLASSIFICATION MODEL

	ACC (%)	PRC (%)	SPC (%)	Recall (%)	F1-score (%)
AK	97.47	91.49	99.01	85.15	88.21
BCC	97.36	85.98	98.14	91.09	88.46
BKL	96.59	88.89	98.76	79.21	83.77
DF	97.80	91.75	99.01	88.12	89.90
HS	98.46	94.85	99.38	91.09	92.93
NV	97.58	85.59	98.02	94.06	89.62
MEL	95.27	76.85	96.91	82.18	79.43
SCC	97.47	86.79	98.27	91.09	88.89
VASC	99.78	100.00	100.00	98.02	99.00
AVG	97.53	89.13	98.61	88.89	88.91

\* AK: Actinic Keratosis, BCC Basal Cell Carcinoma, BKL: Benign Keratosis, DF: Dermatofibroma, HS: Healthy Skin, NV: Melanocytic Nevus, MEL: Melanoma, SCC: Squamous Cell Carcinoma, VASC: Vascular Lesion

The average accuracy of the proposed model obtained is 97.53% on par with the existing work reported in this study. The model detected Vascular lesion with the highest accuracy of 99.78%. The model reported an average precision of 89.13% which is satisfactory considering the large size of data. The average specificity of the model is 98.61%. The model has achieved better specificity than the existing work. The average recall & average F1-score achieved is 88.89% & 88.91% respectively. The proposed model in this system has achieved a better result compared to the existing works.

## C. Comparison with existing work

The findings of the proposed system have been compared with those of existing systems in Table IV. The results show that the accuracy achieved by the proposed system for binary classification is similar to that of existing systems [3], [7], [10]. However, the proposed system has achieved higher sensitivity and specificity compared to the existing systems [3], [4], [10]. The study on the multi-class classification of skin cancer is limited to a maximum of five classes [9], [6], [12], whereas the proposed system has achieved satisfactory results for the multi-class classification of nine classes of skin cancer.



TABLE IV. COMPARISON WITH EXISTING WORK

Authors/Year	Dataset used	Methodology	Evaluation parameter			
			ACC (%)	PRC (%)	SEN (%)	OTHERS
Binary Classification						
L. Ichim et. al. (2020) [7]	PH2	Color HOG- Perceptron, ABCD rule-based classifier, ResNet 101-deep CNN, AlexNet-deep CNN	95	-	-	F1 score = 92%
M.K. Monika et al. (2020) [1]	ISIC 2019 Challenge dataset	ABCD method, GLCM method Multi-class SVM	96.25	96.32	-	-
P. Banasode et. al. (2020) [2]	ISIC dataset	Asymmetric behaviour, colour, and border irregularity SVM	96.9		95.7	SPC = 90.2%
A. A. Adegun et. al. (2019) [3]	ISBI 2017, PH2	Deep Convolutional Encoder-Decoder Networks, Gaussian Filter, Softmax classifier, Lesion classifier	93	-	83	Dice Coefficient = 85% SPC = 97%
Q. Zhou et al (2020) [4]	ISIC 2018 challenge Task 3 dataset	Fast Median Filtering, Univariate Feature Selection, STDP based convolutional SNNs, SVM Classifier	57.7	58.4	53.5	SPC = 61.9 %, AUC = 54%
Jojoa Acosta et al (2021) [10]	ISIC 2017	SVM	90.4	-	82	SPC = 92.5%
M.A. Kadampur et. al. (2020) [8]	HAM10000 dataset	CNN ReLu Resnet50, Densenet201, Squeezenet, InceptionV3	-	-	-	ROC Curve = 99.07%
L. Wei et. al. (2020) [5]	ISBI 2016	MobileNetV1, DenseNet-121 U-MobileNetV1, U-DenseNet121 fusion model	82.9	-	-	AUC= 83%
Proposed work	ISIC 2019	CNN	92.08	88.42	92.25	SPC= 87.92%
Multi-class Classification						
O T Jones et. al. (2022) [9]	Self-Prepared	ABCD score, modified Glasgow 7-point Fotofinder Mole Analyser Pro, DERM, SkinVision,	89.5	-	87	F-1 Score= 88.8%, SPC = 86.4%
Nawal Soliman et. al. (2019) [6]	Self-prepared dataset containing 80 images using multiple resources from the internet	CNN, AlexNet, SVM	100	-	-	-
Z. Yang et. al. (2020) [12]	SIIM-ISIC melanoma dataset	Conversion of BGR, CNN models SVM, RF, KNN, NB	81	-	-	-
Proposed work	ISIC 2019	CNN	97.53	89.13	88.89	F1-score = 88.91%

## V. CONCLUSION

Early detection of Melanoma is essential for both diagnosis and therapy. There is substantial evidence linking UV radiations from sunbeds to development of skin melanoma, Squamous cell carcinoma, and to a lesser amount, basal cell carcinoma, particularly during first exposure which takes place at a younger age. The proposed system detects and classifies the lesion images into cancerous and non-cancerous. If it's cancerous it is categorized into nine different types of skin cancer namely Actinic Keratosis, Benign Keratosis, Melanoma, Basal Cell Carcinoma, Squamous Cell Carcinoma, Dermatofibroma, Melanocytic Nevus, Vascular Lesion, and Healthy Skin. A detailed study of the types, variants, and various treatments of Melanoma is done by referring to various journals and references. The website will act as a useful diagnostic tool for medical practitioners and dermatologists to make more accurate diagnoses, reduce the number of unnecessary biopsies and improve patient outcomes.

The proposed system achieved an average accuracy of 92.08% for binary classification and an average accuracy of 97.53% for multi-class classification. The study done on the multi-class classification of skin cancer is very limited this issue has been addressed by the proposed system which has obtained satisfactory results for the nine-class classification of skin cancer images. Future research can focus on improving the model's performance resulting in a more robust and accurate skin cancer detection system and incorporating more diverse and representative data.

## REFERENCES

- [1] Monika, M. & Kumari, Usha & Kumar, M.N.V.S.S. & Lydia, Laxmi, "Skin cancer detection and classification using machine learning," *Materials Today: Proceedings*, 33, 10.1016/j.matpr.2020.07.366, 2020.
- [2] Praveen Banasode, Minal Patil, & Nikhil Ammanagi "A Melanoma Skin Cancer Detection Using Machine Learning Technique: Support Vector Machine." *IOP Conference Series: Materials Science and Engineering*, 1065(1), 01203, 2021.
- [3] A. A. Adegun and S. Viriri, "Deep Learning-Based System for Automatic Melanoma Detection," in *IEEE Access*, vol. 8, pp. 7160-7172, 2020.
- [4] Q. Zhou, Y. Shi, Z. Xu, R. Qu and G. Xu, "Classifying Melanoma Skin Lesions Using Convolutional Spiking Neural Networks With Unsupervised STDP Learning Rule," in *IEEE Access*, vol. 8, pp. 101309-101319, 2020.
- [5] L. Wei, K. Ding and H. Hu, "Automatic Skin Cancer Detection in Dermoscopy Images Based on Ensemble Lightweight Deep Learning Network," in *IEEE Access*, vol. 8, pp. 99633-99647, 2020.
- [6] Nawal Soliman ALKolifi ALEnezi, "A Method Of Skin Disease Detection Using Image Processing And Machine Learning", *Procedia Computer Science*, Volume 163, 2019, Pages 85-92, ISSN 1877-0509, 2019.
- [7] L. Ichim and D. Popescu, "Melanoma Detection Using an Objective System Based on Multiple Connected Neural Networks," in *IEEE Access*, vol. 8, pp. 179189-179202, 2020.
- [8] Mohammad Ali Kadampur, Sulaiman Al Riyae, "Skin cancer detection: Applying a deep learning based model driven architecture in the cloud for classifying dermal cell images", *Informatics in Medicine Unlocked*, Volume 18, 2020, 100282, ISSN 2352-9148, 2020.
- [9] O. T. Jones et al., "Artificial intelligence and machine learning algorithms for early detection of skin cancer in community and primary care settings: a systematic review," *The Lancet Digital Health*, vol. 4, no. 6. Elsevier BV, pp. e466–e476, Jun. 2022.
- [10] M. F. Jojoa Acosta, L. Y. Caballero Tovar, M. B. Garcia-Zapirain, and W. S. Percybrooks, "Melanoma diagnosis using deep learning techniques on dermoscopic images", *BMC Medical Imaging*, 2021.
- [11] Masood, A. and Ali Al-Jumaily, A., "Computer-aided diagnostic support system for skin cancer: a review of techniques and algorithms." *International journal of biomedical imaging*, 2013.
- [12] Yuan X, Yang Z, Zouridakis G, Mullani N, "SVM-based texture classification and application to early melanoma detection." *Conf Proc IEEE Eng Med Biol Soc.* 2006;2006:4775-8, 2020.
- [13] W. V. Stoecker, M. Wronkiewicz, R. Chowdhury, R. J. Stanley, J. Xu, A. Bangert, et al., "Detection of granularity in dermoscopy images of malignant melanoma using color and texture features", *Comput. Med. Imag. Graph.*, vol. 35, no. 2, pp. 144-147, March 2011.
- [14] M. E. Celebi, H. A. Kingravi, B. Uddin, H. Iyatomi, Y. A. Aslandogan, W. V. Stoecker, et al., "A methodological approach to the classification of dermoscopy images", *Comput. Med. Imag. Graph.*, vol. 31, no. 6, pp. 362-373, 2007.
- [15] <https://www.skincancer.org/skin-cancer-information/>
- [16] C. Bertolotto, "Melanoma: From Melanocyte to Genetic Alterations and Clinical Options", *Scientifica*, vol. 2013, p. 635203, December 2013.
- [17] [https://www.who.int/news-room/questions-and-answers/item/radiation-ultraviolet-\(uv\)-radiation-and-skin-cancer](https://www.who.int/news-room/questions-and-answers/item/radiation-ultraviolet-(uv)-radiation-and-skin-cancer)
- [18] Nasti, T.H. and Timares, L "MC1R, eumelanin and pheomelanin: Their role in determining the susceptibility to skin cancer, Photochemistry and photobiology." U.S. National Library of Medicine, 2015.
- [19] Bailey EC, Sober AJ, Tsao H, Mihm MC, Jr., Johnson TM, Jr.. Chapter 124. "Cutaneous Melanoma." In: Goldsmith LA, Katz SI, Gilchrist BA, Paller AS, Leffell DJ, Wolff K. eds. *Fitzpatrick's Dermatology in General Medicine*, 8e. McGraw Hill; 2012.
- [20] <https://www.aad.org/public/diseases/skin-cancer/actinic-keratosis-treatment>
- [21] Jahnke MN. "Vascular Lesions." *Pediatr Ann.* 1;45(8):e299-305. August 2016.
- [22] McDaniel B, Badri T, Steele RB. Basal Cell Carcinoma. [Updated 2022 Sep 19]. In: StatPearls [Internet]. Treasure Island (FL): StatPearls Publishing; January 2023.
- [23] Greco MJ, Bhutta BS. Seborrheic Keratosis. [Updated 2023 Feb 9]. In: StatPearls [Internet]. Treasure Island (FL): StatPearls Publishing; January 2023.
- [24] <https://emedicine.medscape.com/article/1058445-overview>
- [25] Myers DJ, Fillman EP. Dermatofibroma. [Updated 2022 Oct 24]. In: StatPearls [Internet]. Treasure Island (FL): StatPearls Publishing; January 2023.
- [26] ISIC 2019 Dataset: <https://challenge.isic-archive.com/data/#2019>
- [27] SIIM-ISIC Dataset; <https://www.kaggle.com/competitions/siim-isic-melanoma-classification>
- [28] Jutzi T.B., Krieghoff-Henning E.I., Holland-Letz T., Utikal J.S., Hauschild A., Schadendorf D., Sonderrmann W., Fröhling S., Hekler A., Schmitt M., et al. Artificial Intelligence in Skin Cancer Diagnostics: The Patients' Perspective. *Front. Med.* 2020.